BioArchitecture

ISSN: 1949-0992 (Print) 1949-100X (Online) Journal homepage: http://www.tandfonline.com/loi/kbia20

Organized chaos in Kupffer's vesicle: How a heterogeneous structure achieves consistent left-right patterning

DJ Smith, TD Montenegro-Johnson & SS Lopes

To cite this article: DJ Smith, TD Montenegro-Johnson & SS Lopes (2014) Organized chaos in Kupffer's vesicle: How a heterogeneous structure achieves consistent left-right patterning, BioArchitecture, 4:3, 119-125, DOI: 10.4161/19490992.2014.956593

To link to this article: http://dx.doi.org/10.4161/19490992.2014.956593

Accepted author version posted online: 06 Nov 2014.
Published online: 06 Nov 2014.

Bioarchitecture 4:3, 119–125; May/June 2014; © 2014 Landes Bioscience

Organized chaos in Kupffer's vesicle: How a heterogeneous structure achieves consistent left-right patterning

DJ Smith[1,4,5], TD Montenegro-Johnson[2], and SS Lopes[3,*]

[1]School of Mathematics; University of Birmingham; Birmingham, UK; [2]Department of Applied Mathematics and Theoretical Physics; University of Cambridge; Center for Mathematical Sciences; Wilberforce Road; Cambridge, UK; [3]CEDOC; Faculdade de Ciências Mèdicas; Universidade Nova de Lisboa; Lisboa, Portugal; [4]Centre for Human Reproductive Science; Birmingham Women's; NHS Foundation Trust; Birmingham, UK; [5]School of Engineering and Center for Scientific Computing; University of Warwick; Coventry, UK

Successful establishment of left-right asymmetry is crucial to healthy vertebrate development. In many species this process is initiated in a ciliated, enclosed cavity, for example Kupffer's vesicle (KV) in zebrafish. The microarchitecture of KV is more complex than that present in the left-right organizer of many other species. While swirling flow in KV is recognized as essential for left-right patterning, its generation, nature and conversion to asymmetric gene expression are only beginning to be fully understood. We recently [Sampaio, P et al. Dev Cell 29:716–728] combined imaging, genetics and fluid dynamics simulation to characterize normal and perturbed ciliary activity, and their correlation to asymmetric charon expression and embryonic organ fate. Randomness in cilia number and length have major implications for robust flow generation; even a modest change in mean cilia length has a major effect on flow speed to due to nonlinear scaling arising from fluid mechanics. Wildtype, and mutant embryos with normal liver laterality, exhibit stronger flow on the left prior to asymmetric inhibition of charon. Our discovery of immotile cilia, taken with data on morphant embryos with very few cilia, further support the role of mechanosensing in initiating and/or enhancing flow conversion into gene expression.

Keywords: cilia, heterotaxia, Kupffer's vesicle, left-right asymmetry, situs inversus, zebrafish

Abbreviations: DA, dorsal roof-anterior; DC, dorsal roof-central; DP, dorsal roof-posterior; dld$^{-/-}$, homozygous deltaD null mutant; dnah7-MO, dnah7-morpholino knockdown embryo; EQ, equatorial region of Kupffer's vesicle separating dorsal roof and ventral floor; KV, Kupffer's vesicle; MO-control, embryo treated with mismatch control morpholino; VA, ventral floor-anterior; VC, ventral floor-central; VP, ventral floor-posterior; WT, wildtype

*Correspondence to: SS Lopes; Email: susana.lopes@fcm.unl.pt

Submitted: 08/07/2014

Accepted: 08/16/2014

http://dx.doi.org/10.4161/19490992.2014.956593

Background

Left-right symmetry breaking occurs in development after the establishment of the anterior-posterior and dorsal-ventral axes. Situs solitus, the normal placement of left heart and (in zebrafish, but not human) left liver, results from the left-right axis breaking in a consistent way.

The importance of cilia-driven flow in a transient organizing structure in this consistent breaking of left-right symmetry was first discovered in mouse,[1,2] and subsequently in the zebrafish.[3] In mouse, the organizing structure is the node, a fluid-filled cavity on the ventral side of the embryo, appearing at around embryonic day 8 (e.7.75). The architecture of the mouse node is relatively simple—a flat-floored pit-like depression with a flat epithelium, that expresses whirling cilia. These cilia are tilted toward the already-existing posterior axis, and the combination of tilt, and preferred whirling chirality, clockwise when viewed tip-to-base, produces a leftward flow, as first predicted by Cartwright et al.[4] and subsequently observed experimentally.[5-7]

The viscous fluid mechanics underlying flow generation by tilted whirling cilia were discussed by Nonaka et al.[5] and Brokaw,[8] and explored through models and simulation by Smith et al.[9] and Cartwright et al.[10] The microscopic size of the cilia entails that the fluid flow regime has a very low Reynolds number, so that viscous effects dominate inertia. The flow regime of a whirling cilium is therefore more akin to slow motion through a thick oil or syrup than the turbulent mixing of soup in a blender. Indeed this dynamic similarity was modeled experimentally[5] through tracking glitter transport in silicone oil driven by tilted slowly-rotating wires.

The motion of the cilium can be considered as consisting of 2 phases, leftward and rightward. The chirality of the beat, combined with the posterior tilt, means that the cilium is farther from the epithelial surface during the leftward phase than the rightward phase. Viscous drag due to the surface is greater during the rightward motion than leftward, resulting in an overall leftward motion above the cilia tips.

Perhaps counterintuitively, a particle suspended in the flow is not simply 'streamed' to the left, but rather undergoes a 'loopy drift'. In what follows, 'leftward flow' should be interpreted as an overall leftward loopy drift of particles rather than a steady streaming of fluid. Other more complex features of particle motion in nodal flow include trapping-and-release of particles close to the epithelium,[2,9] and the transition from rotational to directional flow moving from near to far field.[11,12] Leftward transport in and near the ciliated surface is balanced by rightward transport in the upper region of the node, resulting from the sealing of the cavity by Reichert's membrane, and consequent mass-conserving counterflow.[4]

The architecture of Kupffer's vesicle (KV) of zebrafish is somewhat more complex, and involves the interplay of several mechanisms. Our recent study[13] combined genetic manipulation, imaging and simulation to probe how the arrangement and motility of cilia generates flow, and what features of the flow are associated with situs solitus. Before discussing our new data, we briefly review prior knowledge of the microstructure of KV and its symmetry-breaking flow.

KV is an ellipsoidal fluid-filled cavity that appears around 12 hours post fertilization in the zebrafish embryo (**Fig. 1A, B**). Unlike the mammalian node, KV is enclosed by curved ciliated epithelial surfaces on all sides (**Fig. 1C–E**) rather than having the relatively flat epithelium of mouse and overlying Reichert's membrane. Moreover, the flow structure is less easily characterized as a simple 'leftward' flow, as revealed by Kreiling et al.[14] and Supatto et al.[11] instead involving a swirling motion when visualised in the coronal midplane (**Fig. 1F, G**). Nevertheless, cilia do appear to perform a tilted rotational motion, as in the mouse embryo (**Fig. 1H**), the hydrodynamic interaction associated with the tilt producing flow.

Instead of the ciliated nodal floor and overlying membrane, KV can be considered as consisting of a dorsal roof, ventral floor, and in addition an 'equatorial' region in between (**Fig. 1I–K**). Our study focused on imaging flow in the coronal midplane equidistant from dorsal roof and ventral floor. Previously, studies showed[11,14,15] a 'swirling' flow in the anticlockwise direction when viewed from dorsal, with higher fluid velocity at the anterior end, visualized in our work by tracking native KV particles.

Interpreting how whirling cilia motion produces the observed swirling flow in the midplane is more complex than interpreting leftward flow in the mouse. Simulation[16] provides a tool to explore the consequences of theoretical models. Both the dorsal roof and ventral floor are ciliated: if cilia were equally distributed on the roof and floor, the 'mirror image' motions would cancel out in the midplane. Several studies[11,14,15] have confirmed cilia are denser on the dorsal roof than the ventral floor, and denser at the anterior end of the dorsal roof in particular (**Fig. 1E, I**); this clustering occurs due to KV cell shape remodelling involving the Rock2b-Myosin II pathway.[17] Kreiling et al.[14] also reported posterior tilt of these cilia. Simulations have shown[16] how tilted whirling cilia, which generate locally a dominant flow at right angles to the tilt direction (**Fig. 1H**), arranged in an dorsal roof-anterior clustering, act together to produce an overall swirling flow in the midplane. We can consider the dorsal roof-anterior (DA), and also the ventral floor-posterior (VP) regions as effective, in the sense that they positively contribute to the chiral swirl. By contrast, the dorsal roof-posterior (DP) and ventral floor-anterior (VA) regions are reversing, in the sense that they oppose the chiral swirl. Under this model, effective flow is produced due to the DA and VP cilia outnumbering the DP and VA cilia (**Figs. 1I, K**).

Another effect crucial in generating flow was reported by Supatto et al.:[11] dorsal tilt, in particular in equatorially-located cilia (**Fig. 1J**). In this region, all cilia contribute to the swirling flow, so we denote dorsally-tilted equatorial cilia as also being effective. Though dorsal-only tilt has been shown via simulation[16] to be sufficient to generate swirling midplane flow, clustering of posterior-tilted cilia in the DA region augments the strength of this flow, suggesting a role for both types of tilt in zebrafish KV. An interesting finding from formulating a geometric model is that at the dorsal-anterior region, posterior tilt and dorsal tilt directions are similar, and may be difficult to distinguish experimentally.

Cilia numbers in the mouse node are 200–300 in wildtype,[18] however as few as 2 cilia are capable of breaking left-right symmetry.[19] Therefore we asked the question, how many cilia are sufficient to generate a flow field capable of generating situs solitus? As opposed to the highly robust mammalian system, even wildtype KVs fail to achieve situs solitus in around 10% of cases. Moreover, cilia numbers, length and location show considerable variability, and the distribution of cilia is relatively sparse. To examine and quantify the effect of this heterogeneity, we explored a combined approach involving genetic manipulation, imaging, and theoretical modeling involving both statistical sampling and fluid mechanics simulation. First we discuss the statistical aspects of our data on KV architecture.

Unexpected heterogeneity of the KV cilia population

Previous work[20] has shown that zebrafish KV cilia in wildtype vary in length, with most being 3–5 μm in length, with counts of around 50–60 cilia.[21] In our recent study using a larger sample of 27 WT embryos (639 cilia in total) we noticed that the range of cilia length (measured in 3D) and cilia numbers were surprisingly large, being 2–9 μm (mode 4.5 μm) and 10–75 cilia (mode 30 cilia). We also measured motility and cilia beat frequency, and found that while approximately 60% exhibited a relatively simple beat characterized by a single Fourier mode, around one fifth were immotile, the remaining fifth appeared to perform a more complex motion, with 2 frequency peaks. We referred to the latter as 'wobbling' cilia, and suggest that oscillation in the cone angle may be responsible

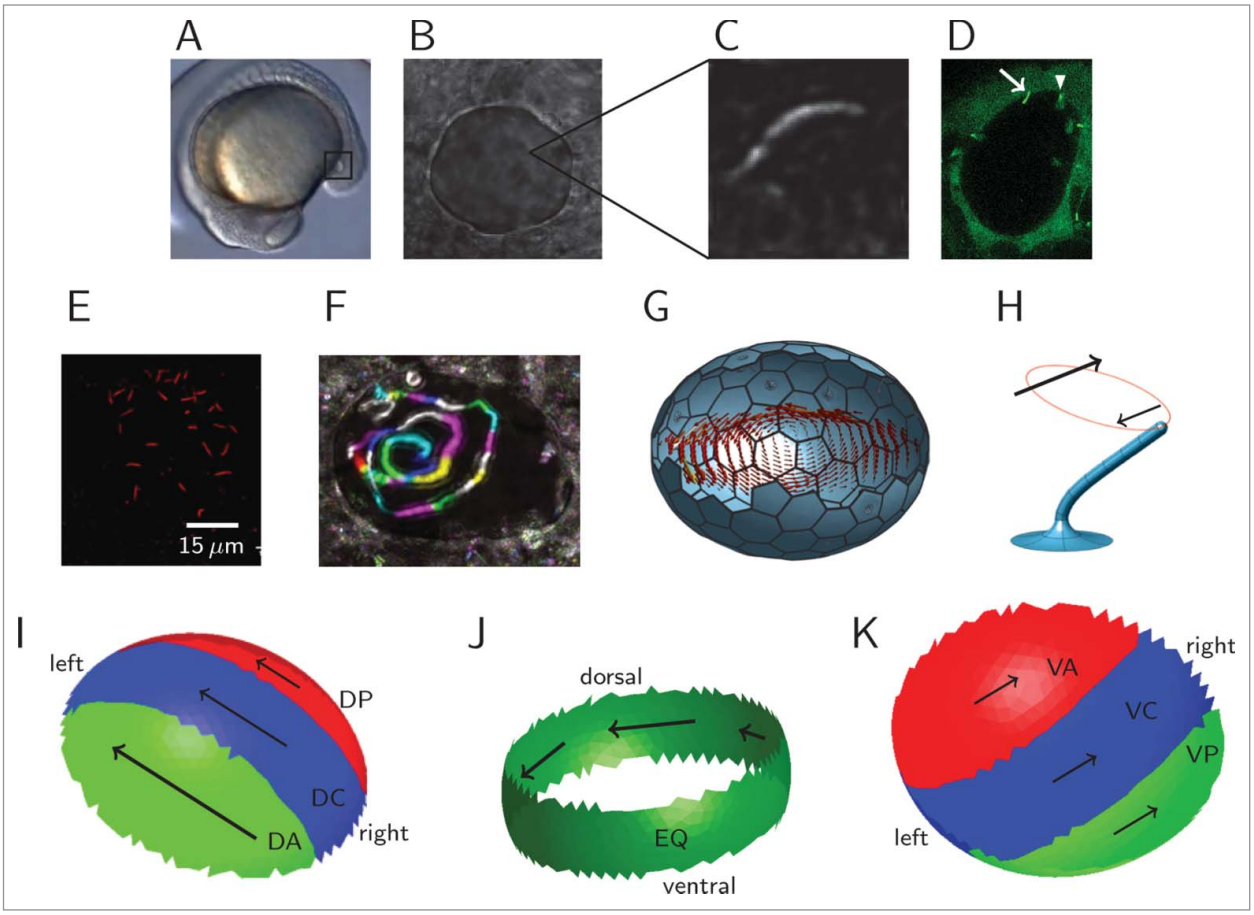

Figure 1. Kupffer's vesicle and cilia population, and the generation of swirling fluid flow. (**A**) Location of the KV (highlighted with a square) in a zebrafish embryo at 14 hours post fertilization. (**B**) Image of KV in a live embryo—'left' is to the left and anterior to the top unless stated, with (**C**) showing a background-subtracted image of a KV cilium. (**D**) Fluorescence image at 14 hpf with both cilia and cells labeled with GFP. Immotile cilia appear sharp (indicated with an arrow), whereas motile cilia appear as cones due to motion blur (indicated with an arrowhead). (**E**) Immunofluorescence staining to indicate anterior cilia clustering in a wildtype embryo. (**F**) Representative particle flow map in wildtype, with color sequence being used to indicate the progression of time. (**G**) Image of a full ciliated wildtype mesh with computed swirling midplane flow profile from simulation. (**H**) Image from a computational mesh of a model cilium, indicating the tilt and rotational trajectory. The larger arrow indicates the greater flow produced by the upper portion of the stroke than the lower portion, perpendicular to the tilt direction. (**I, J, K**) schematics of the effective (green), neutral (blue) and reversing (red) regions of KV, looking at (**I**) the interior surface of the dorsal roof, (**J**) the equatorial region, (**K**) the interior side of the ventral floor. Arrow lengths indicate relative flow speeds associated with cilia density. (**A–H**) reprinted from ref.[13] with kind permission, copyright 2014 Elsevier.

for producing this additional peak. The immotile cilia may be dynamically significant for 2 reasons: first, they do not contribute to flow, so in phenotypes with few cilia 'to spare', the loss of an additional fifth may result in a critical reduction in flow. It is therefore essential to distinguish total and motile cilia when characterizing a phenotype by cilia number. Second, the immotile cilia may, as is believed in other species,[18,22] act to sense the flow mechanically. Further evidence for this idea was revealed by gene expression data; first however we will review the implications of this randomness for flow generation.

The numbers game: how randomness influences development

An existing fluid dynamical model[16] resolved at the scale of single cilia was adapted to allow for random placement of immotile cilia, random cilia lengths and frequencies according to our data. Five simulations were performed for model WT embryos with each of 25, 37, 48 and 60 cilia and dld$^{-/-}$ mutant embryos with 15, 22, 29 and 36 cilia (40 simulations in total) to examine how the flow fields within KV with different cilium numbers are affected by the observed variations. Cilia were randomly placed on the inner surface of KV using the cilium density distributions previously reported[14,20] of 38% in the dorsal-anterior corner, 25% in the dorsal central-region, 17% in the dorsal-posterior corner and the remaining 20% on the dorsal floor. Frequencies, lengths and motility were then randomly assigned to these cilia by sampling from distributions fitting our experimental data—for example the gamma distributions for cilia length in **Figure 2G**. The effect of randomness, especially immotility, is proportionally greater in embryos with fewer cilia than with more cilia. Fluid dynamic simulations showed progressively clearer

dominance of both the anterior and left-sided flow velocities with higher cilia numbers in both WT and dld$^{-/-}$.

Fully resolved fluid dynamics simulations give insight into the flow within KV, but each simulated KV requires several hours of CPU time for the computation to complete. A simpler approach to gain insight into the effect of cilia numbers which we will use in this commentary can be gained by creating a coarse-grained statistical model to examine the natural variation in the placement of motile and immotile cilia for vesicles as a function of the total number of cilia. **Figure 2A–E**

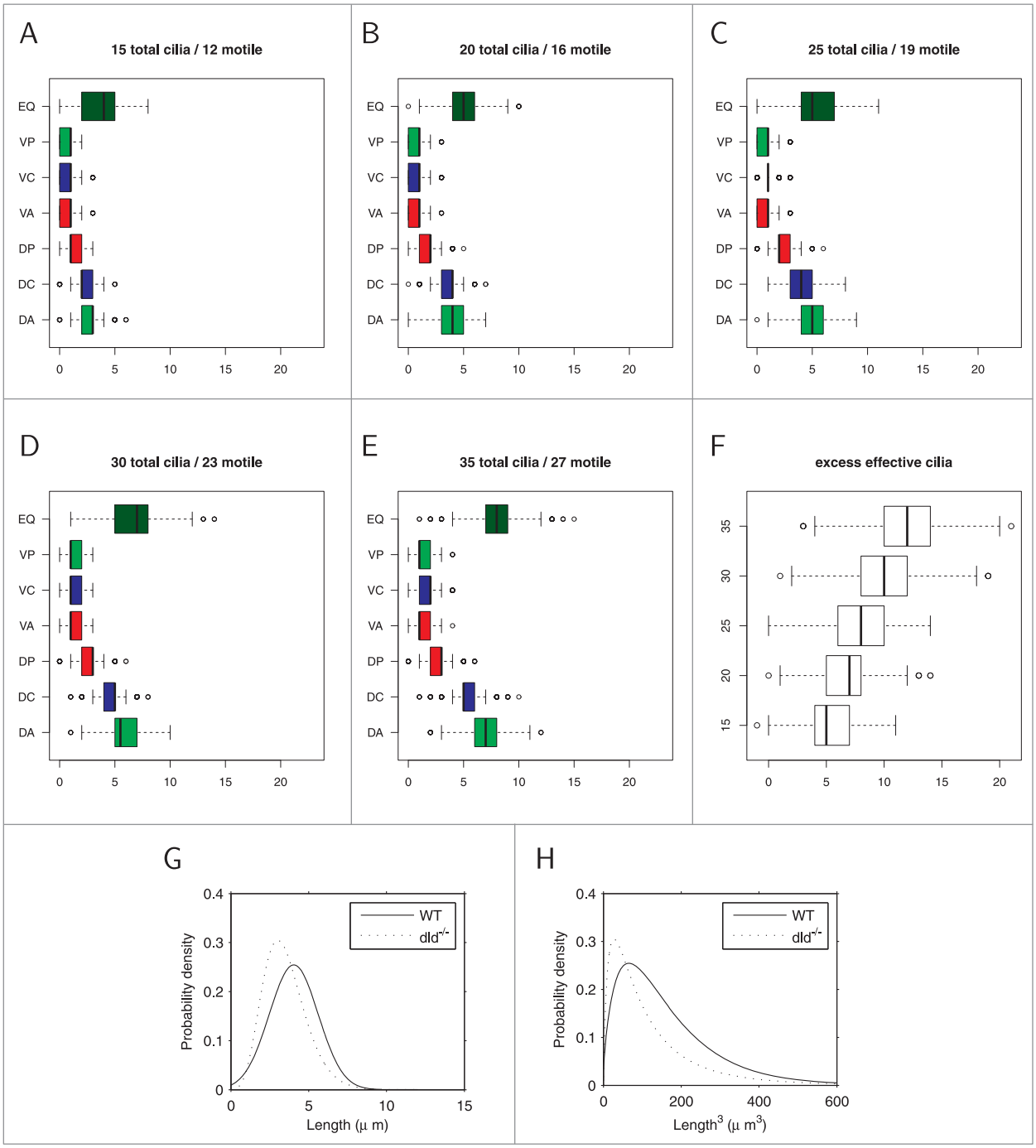

Figure 2. Statistical effects of modifications to cilia numbers and lengths in wildtype and mutants, calculated from the models in ref.[13]. (**A, B, C, D, E**) statistical sampling results for a total of 5000 randomly-generated 'virtual KVs' with respective populations of 15, 20, 25, 30, and 35 cilia, showing numbers of cilia in each region (color coded to match **Fig. 1**). (**F**) the excess effective motile cilia able to contribute to the swirl (green minus red) for each population size. (**G**) gamma distributions of cilia length for wildtype and dld$^{-/-}$ mutant fitted to experimental data, (**H**) corresponding probability density functions for (length) 3 in wildtype and dld$^{-/-}$ mutant, as an indication of the volume flow rate produced by each tilted whirling cilium.12

show the outcome of sampling 1000 virtual KV for each of 15, 20, 25, 30, and 35 cilia from the statistical model used by Sampaio et al.[13] showing the distributions of cilia in each region described above (green denoting effective and red reversing regions), with the excess effective cilia for each number being shown in **Figure 2F**. For KVs possessing the wildtype mode of 30 cilia, the 10th percentile for excess motile cilia is 6. Recalling that 90% of WT KVs achieve situs solitus suggests that normal swirling flow and resulting situs solitus is produced by relatively few excess effective cilia.

From monitoring embryo fates we know that approximately 60% of dld$^{-/-}$ mutants achieve situs solitus.[20] This reduction is in part due to the reduction in motile cilia numbers in the dld$^{-/-}$mutant: the modal cilia number is 15, and half of the 15-cilia KVs sampled had 5 or fewer excess motile cilia. Another effect is perhaps even more important in impairing the organizing flow in dld$^{-/-}$ mutants: fluid dynamical analysis of whirling cilia[12] suggests a cubic dependence of cilia-driven transport on cilia length. The effect of this nonlinear dependence is evident in both simulations and observations of the short cilia dld$^{-/-}$ mutant;[20] we therefore consider the effect over the length distributions we fitted to WT and dld$^{-/-}$data in figure 2G. While the WT and dld$^{-/-}$ length probability density functions have relatively similar means (4.04 μm and 3.49 μm respectively), the probability density functions for (length)^3 have a pronounced difference in means (96.3 μm^3 and 64.3 μm^3 respectively) in addition to a clearly greater spread (**Fig. 2H**). Taking the above together, we therefore see that the dld$^{-/-}$ mutant therefore experiences a 'double-hit' of both a smaller excess of effective cilia, and an average of one third less flow produced by each cilium; the outcome is that situs solitus only occurs in 60% of embryos. Nevertheless, WT embryos do not achieve near-perfect situs when considered collectively; rather in most cases (90%) WT produces sufficiently many cilia to tip the balance in favor of situs solitus. An interesting additional consequence of this nonlinear dependence is that longer cilia have a disproportionately large influence on the flow wherever they occur, further amplifying the effect of length heterogeneity on flow. We now turn to discuss perhaps the most vital aspect of this system, the link between flow and asymmetric gene expression.

Left-right asymmetry of flow speed and the connection between heart and gut situs

Building on the established finding that anterior-posterior asymmetry in the

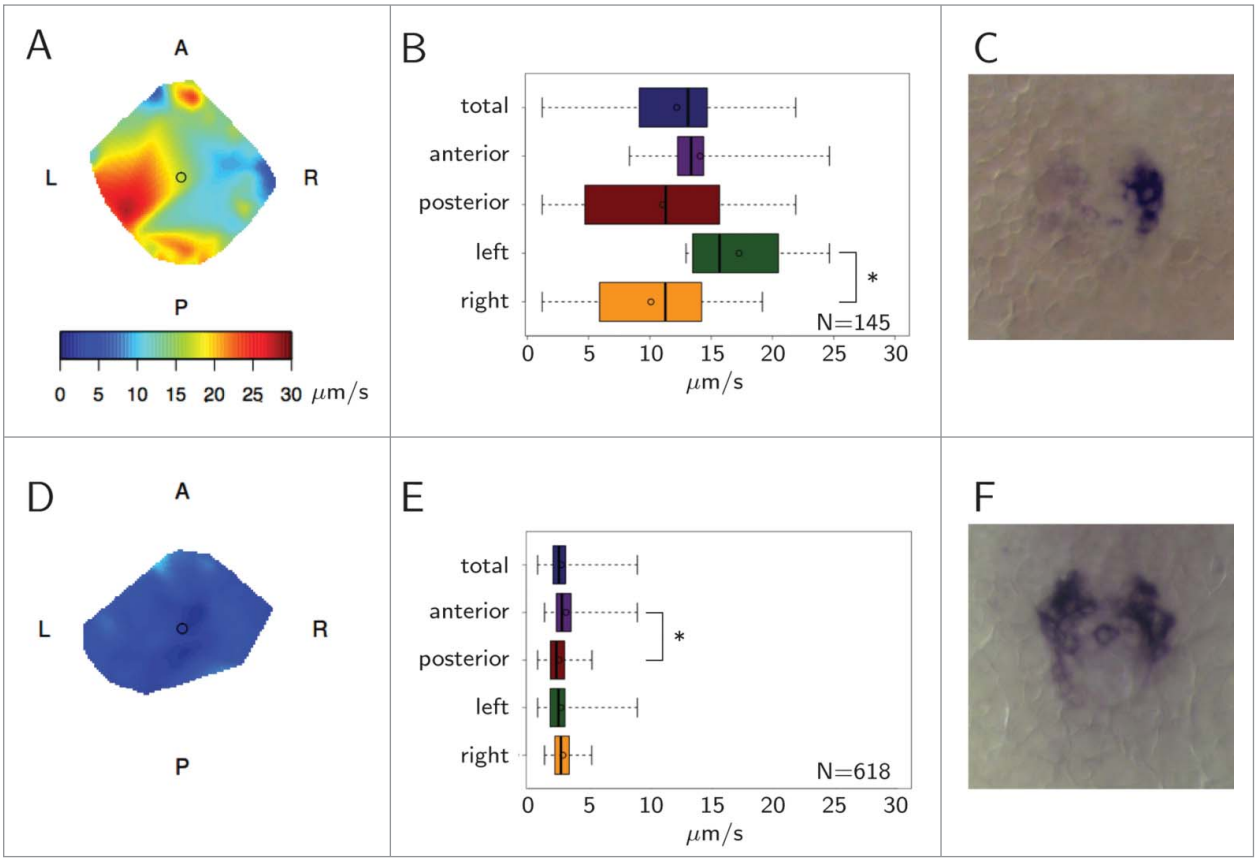

Figure 3. Flow speed characteristics and gene expression. Example wildtype KV with faster flow on the left shown as (**A**) heat map and (**B**) boxplot (asterisk denotes $P < 0.05$). Expression of charon (**C**) is clearly suppressed on the left side. Example dnah7-MO with nearly absent flow is shown as (**D**) heat map and (**E**) boxplot. Expression of charon (**F**) is approximately symmetric. Reprinted from ref.[13] with kind permission, copyright 2014 Elsevier.

flow speed is important to situs solitus, we found that flow velocity is also left-right asymmetric prior to asymmetric charon expression (**Fig. 3A–C**), an effect that was also reproduced by many simulations, particularly those with greater than 30 cilia. Tracking experiments with native KV particles showed that flow on the left of KV was significantly larger than on the right in WT, and also in the $dld^{-/-}$ mutants which eventually showed left livers. Heterotaxic $dld^{-/-}$ embryos with left heart and right liver showed the expected anterior-posterior, but not left-right flow asymmetry. Finally, heterotaxic $dld^{-/-}$ embryos with central guts showed no significant differences either anterior-posterior or left-right. These findings suggest a sequential process: faster anterior flow initiates left-right asymmetry, resulting in a left heart, and potentially left-right asymmetric cilia activity, resulting in left-right asymmetric flow, charon inhibition on the left, and finally left liver.

dnah7 morphants with very few motile cilia typically exhibited very weak flow and symmetric charon expression (**Fig. 3D–F**). However, 5 out of 6 embryos with a very small number of motile cilia clustered together on either the left or the right exhibited lack of charon expression concordant with cilia location. This experiment highlighted the important role of local flow in a very low background flow scenario, and recapitulates the recent discovery that 2 cilia are enough to break symmetry into situs solitus.[19] We must however add the following qualification: 2 cilia can cause asymmetric gene expression, but only if they are in the correct location.

Conclusions

Through a combination of imaging, genetics and modeling, we found that KV is more of a biasing than robust organizer, achieving normal situs most of the time, despite wide natural variation of total numbers and lengths of flow-generating cilia and associated variability in the flow fields. In KV with fewer than approximately 30 cilia, random variations in ciliation patterns and lengths may result in insufficient dominance of the anterior flow, and hence heterotaxia or situs inversus. The modal value of 30 cilia observed in WT provides a strong enough balance of effective to reversing cilia for situs solitus to occur in the majority of embryos; the balance in favor of effective cilia may however be an excess number of just 6. Cilium length is also very important in the physics of flow generation; a modest reduction in the $dld^{-/-}$mutant results in a pronounced reduction in flow via a cubic scaling law. We observed a broad range of flow velocities experimentally, a behavior also reproduced in our simulations; this heterogeneous flow is just consistent enough to ensure correct left-right organization in the majority of embryos, motivating our use of the term 'organized chaos'.

Virtual KV produced through statistical sampling, and associated fluid mechanics simulation, aided with quantifying the range of flows that may exist in nature without exhaustive experimentation; this approach also required us to make quantitative our conceptual understanding of KV architecture, and in turn enabled the consequences of these models to be verified against data. An unexpected finding of the fluid mechanics model was that left-dominant flow can occur from a symmetric specification of cilia. Simplified approaches, perhaps in the spirit of the rotlet array of Cartwright et al.[4] may provide insight into how this phenomenon arises in the more complicated setting of the zebrafish organizer.

An important insight from our work with heterotaxic embryos was the notion of sequential flow events. For situs solitus, the anterior flow is a prerequisite, followed by faster left-sided flow and charon mRNA degradation. By noticing that $dld^{-/-}$ embryos had anterior faster flow but lacked left-biased flow, we have uncoupled the biophysical events that lead to the disconnection of heart and gut situs. Heterotaxia may be more complex to explain in mammals; we however hope that this study will aid the design of future fish and mammal nodal flow experiments and their interpretation.

Disclosure of Potential Conflicts of Interest

No potential conflicts of interest were disclosed.

Acknowledgments

We thank our co-authors, Pedro Sampaio, Rita Ferreira, Adán Guerrero, Petra Pintado, Bárbara Tavares, Joana Amaro and Andrew Smith.

Funding

SSL was supported by Fundação para a Ciência e a Tecnologia (FCT) SFRH/BPD/34822/2007 and FCT Investigator contract.

References

1. Sulik K, Dehart DB, Inagaki T, Carson JL, Vrablic T, Gesteland K, Schoenwolf GC. Morphogenesis of the murine node and notochordal plate. Am J Anat 1994; 201(3):260-78.
2. Nonaka S, Tanaka Y, Okada Y, Takeda S, Harada A, Kanai Y, Kido M, Hirokawa N. Randomization of left-right asymmetry due to loss of nodal cilia generating leftward flow of extraembryonic fluid in mice lacking KIF3B motor protein. Cell 1998; 95(6):829-37; PMID:9865700; http://dx.doi.org/10.1016/S0092-8674(00)81705-5
3. Kramer-Zucker AG, Olale F, Haycraft CJ, Yoder BK, Schier AF, Drummond IA. Cilia-driven fluid flow in the zebrafish pronephros, brain and Kupffer's vesicle is required for normal organogenesis. Development 2005; 132(8):1907-21; PMID:15790966; http://dx.doi.org/10.1242/dev.01772
4. Cartwright JHE, Piro O, Tuval I. Fluid-dynamical basis of the embryonic development of left-right asymmetry in vertebrates. Proc Natl Acad Sci USA 2004; 101 (19):7234-9; PMID:15118088; http://dx.doi.org/10.1073/pnas.0402001101
5. Nonaka S, Yoshiba S, Watanabe D, Ikeuchi S, Goto T, Marshall WF, Hamada H. De novo formation of left-right asymmetry by posterior tilt of nodal cilia. PLoS Biol 2005; 3(8):1467-72; http://dx.doi.org/10.1371/journal.pbio.0030268
6. Tanaka Y, Okada Y, Hirokawa N. FGF-induced vesicular release of Sonic hedgehog and retinoic acid in leftward nodal flow is critical for left–right determination. Nature 2005; 435(7039):172-7; PMID:15889083; http://dx.doi.org/10.1038/nature03494
7. Hirokawa N, Okada Y, Tanaka Y. Fluid dynamic mechanism responsible for breaking the left-right symmetry of the human body: the nodal flow. Annu Rev Fluid Mech 2009; 41:53-72; http://dx.doi.org/10.1146/annurev.fluid.010908.165141
8. Brokaw CJ. Computer simulation of flagellar movement IX Oscillation and symmetry breaking in a model for short flagella and nodal cilia. Cell Motil Cytoskeleton 2005; 60(1):35-47; PMID:15573415; http://dx.doi.org/10.1002/cm.20046
9. Smith DJ, Gaffney EA, Blake JR. Discrete cilia modelling with singularity distributions: application to the embryonic node and the airway surface liquid. Bull Math Biol 2007; 69(5):1477-510; PMID:17473955; http://dx.doi.org/10.1007/s11538-006-9172-y
10. Cartwright JHE, Piro N, Piro O, Tuval I. Embryonic nodal flow and the dynamics of nodal vesicular parcels. J R Soc Interface 2007; 4(12):49-55; PMID:17015289; http://dx.doi.org/10.1098/rsif.2006.0155
11. Supatto W, Fraser SE, Vermot J. An all-optical approach for probing microscopic flows in living embryos. Biophys J 2008; 95(4):29-31; http://dx.doi.org/10.1529/biophysj.108.137786
12. Smith DJ, Blake JR, Gaffney EA. Fluid mechanics of nodal flow due to embryonic primary cilia. J R Soc Interface 2008; 5(22):567-73; PMID:18211867; http://dx.doi.org/10.1098/rsif.2007.1306

13. Sampaio P, Ferreira RR, Guerrero A, Pintado P, Tavares B, Amaro J, Smith AA, Montenegro-Johnson TD, Smith DJ, Lopes SS. Left-right organizer flow dynamics: how much cilia activity reliably yields laterality? Dev Cell 2014; 29:716-28; PMID:24930722; http://dx.doi.org/10.1016/j.devcel.2014.04.030
14. Kreiling JA, Prabhat, Williams G, Creton R. Analysis of Kupffer's vesicle in zebrafish embryos using a Cave automated virtual environment. Dev Dyn 2007; 236 (7):1963-9; PMID:17503454; http://dx.doi.org/10.1002/dvdy.21191
15. Okabe N, Xu B, Burdine RD. Fluid dynamics in zebrafish Kupffer's vesicle. Dev Dyn 2008; 237(12):3602-12; PMID:18924242; http://dx.doi.org/10.1002/dvdy.21730
16. Smith AA, Montenegro-Johnson TD, Smith DJ, Blake JR. Symmetry breaking cilia-driven flow in the zebrafish embryo. J Fluid Mech 2012; 705:26-45; http://dx.doi.org/10.1017/jfm.2012.117
17. Wang G, Manning ML, Amack JD. Regional cell shape changes control form and function of Kupffer's vesicle in the zebrafish embryo. Dev Biol 2012; 370(1):52-62; PMID:22841644; http://dx.doi.org/10.1016/j.ydbio.2012.07.019
18. Freund JB, Goetz JG, Hill KL, Vermot J. Fluid flows and forces in development: functions, features and biophysical principles. Development 2012; 139(7):1229-45; PMID:22395739; http://dx.doi.org/10.1242/dev.073593
19. Shinohara K, Kawasumi A, Takamatsu A, Yoshiba S, Botilde Y, Motoyama N, Reith W, Durand B, Shiratori H, Hamada H. Two rotating cilia in the node cavity are sufficient to break left-right symmetry in the mouse embryo. Nat Comms 2012; 3:622; PMID:22233632; http://dx.doi.org/10.1038/ncomms1624
20. Lopes SS, Louren Rço, Pacheco L, Moreno N, Kreiling J, Saúde L. Notch signalling regulates left-right asymmetry through ciliary length control. Development 2010; 137(21):3625-32; PMID:20876649; http://dx.doi.org/10.1242/dev.054452
21. Amack JD. Salient features of the ciliated organ of asymmetry. BioArchitecture 2014; 4:6-15; PMID:24481178; http://dx.doi.org/10.4161/bioa.28014
22. Yoshiba S, Shiratori H, Kuo IY, Kawasumi A, Shinohara K, Nonaka S, Asai Y, Sasaki G, Belo JA, Sasaki H, et al. Cilia at the node of mouse embryos sense fluid flow for left-right determination via Pkd2. Science 2012; 338(6104):226-31; PMID:22983710; http://dx.doi.org/10.1126/science.1222538